Pressure-assisted microwave sintering: A rapid process to sinter submicron sized grained MgAl2O4 transparent ceramics

Gabriel Kerbart, Christelle Harnois, Christelle Bilot, Sylvain Marinel

Pressure-Assisted Microwave Sintering: A Rapid Process to Sinter Submicron sized Grained $MgAl_2O_4$ Transparent Ceramics.

Gabriel Kerbart[1], Christelle Harnois[1], Christelle Bilot[1], Sylvain Marinel[1]

[1] Normandie Univ, ENSICAEN, UNICAEN, CNRS, CRISMAT, 14000 Caen, France

Abstract

This work focuses on the development of an original process based on a 2.45 GHz single-mode microwave cavity equipped with a uniaxial press, to sinter transparent spinel $MgAl_2O_4$ ceramic in air. The samples were conventionally pre-sintered to a density of 90% TD before microwave sintering to the final stage of densification. The influence of thermomechanical cycle on the material properties was investigated. Transmittance, grain size distribution, hardness and fracture toughness of the samples were measured and correlated to the microstructure. This new sintering process has allowed obtaining transparent samples with sub micrometric grain size and high mechanical properties, with relatively short times and low temperature. These first results can be compared to some obtained by SPS or HIP. The technical input of this method is that all the process is here conducted in air atmosphere.

Keywords: Microwave; Uniaxial pressure; Sintering; Transparent Ceramics; Spinel

1. Introduction

Transparent polycrystalline ceramics have attracted much interest from the scientific community but also from industry due to their numerous potential applications in laser host, jewelry, spacecraft windows or IR windows and dome for military applications [1]. These ceramics are characterized by their attractive thermo-mechanical properties from room to high temperature (>1000°C), their intrinsic transparency in the visible-IR range, and the low cost of the raw materials [2]. However, the transparency can only be achieved for highly pure and fully dense materials. In the case of the magnesium aluminate spinel ($MgAl_2O_4$), hereafter termed spinel, this high density can only be achieved with high sintering temperature coupled with mechanical pressure. Techniques such as High Isostatic Pressure (HIP) and Spark Plasma Sintering (SPS) are the most effective in that way.

In the literature, the best results obtained by HIP require the use of a pre-treatment such as conventional sintering or hot forging [3, 4]. For instance, with a conventional pre-sintering step followed by a HIP sintering at 1400°C, Krell et al. [3] obtained transparent spinel, exhibiting 81-85% RIT at 640 nm, with a grain size of 400-600 nm, hardness of 15 GPa and fracture toughness of 2 $MPa.m^{1/2}$. A similar grain size has been obtained by Goldstein et al. [5] on spinel sintered at 1320°C - 170MPa. They measured a transmittance value of 75% RIT at 550 nm with similar mechanical properties.

Transparent spinel has been obtained using SPS at 1300°C-80 MPa by Morita et al. [6]. They reported a grain size of 450 nm, a RIT value of 47% at 550 nm, and a hardness of 15GPa. Bonnefont et al. [7] communicated the production of a transparent ceramic with a mean grain size of 275 nm,

exhibiting 74% RIT at 550 nm and 15 GPa hardness using SPS technique 1300 °C-72 MPa. Sokol et al. [8] obtained a nanosized grains transparent spinel, with a mean grain size of 50 nm, by HPSPS at 1000 MPa and 1000°C, presenting >80% RIT at 550 nm, 18 GPa hardness, and 2.66 MPa.$m^{1/2}$ fracture toughness.

However, those methods involve specific atmosphere conditions during sintering (argon pressure or vacuum in contact with graphite, for respectively HIP and SPS). Otherwise, SPS samples may be contaminated by carbon, which is not favorable to obtain high transparency [9,10]. Therefore, both methods may lead to transparent ceramics with a slight coloration, due to partial reduction [11, 12].

Over the years, microwave energy has emerged as an efficient technology for the synthesis and sintering of oxide ceramics, such as spinel [13], $BaTiO_3$ [14], $CaCu_3Ti_4O_{12}$[15] etc. This process offers a greener alternative to conventional heating, with a faster heating rate and less energy consumption than infrared radiation heating, while working under air. Furthermore, since the penetration depth of the microwave electrical field is a few centimeters in a lot of dielectric materials, it allows a volumetric heating, resulting in an efficient heating technology with a homogenous temperature distribution within the sample [16]. However, as previously evoked, removing all the porosity not only requires the diffusion activation at high temperature (natural sintering) but also high pressure. This is the reason why an original dielectric microwave heating process equipped with a uniaxial press has been developed. This paper aims at presenting this process and the results obtained for the sintering of spinel under uniaxial pressure. A 2.45 GHz single-mode cavity was used and specifically designed to be able to apply a uniaxial pressure during sintering. The overall system will be described and the microstructure, the mechanical and optical properties of the final sintered products will be correlated to the processing conditions.

2. Experimental procedure

2.1. Hot press microwave furnace

Microwaves are produced by a 2.45 GHz microwave generator (Sairem GMP 20KSM) and are transmitted to the resonant cavity through a normalized TE10 rectangular waveguide, ended by a TE_{10m} cavity (m=3 or 4). The cavity is tuned to TE_{103} with the coupling iris, so that the heating is provided by the interactions of the material with the E-field (E-field mode). TE103 resonance conditions are achieved by using a coupling iris and a movable short circuit piston, while the impedance matching is tuned by a waveguide hybrid junction with two short circuit pistons (magic T). The microwave generator can deliver a maximum power of 2 kW. The overall system is shown on figure 1.

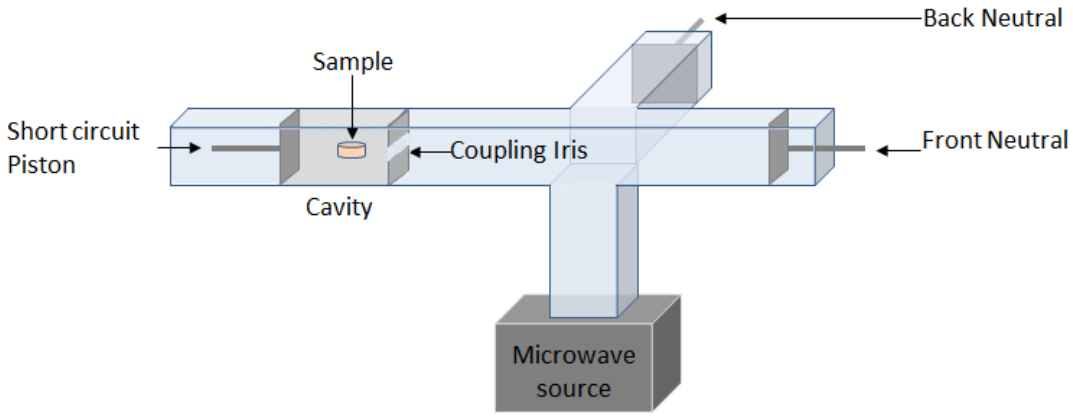

Fig. 1.Scheme top view of the 2.45 GHz microwave furnace

The temperature is measured by an infrared pyrometer (OPTRIS CTM-3SF75H3-C3) pointing on the center of the cavity from its backside, where the sample will be located. This heating system is coupled with a uniaxial press positioned above the cavity. The force is applied by the upper steel punch onto the sample placed between two alumina cylinders to avoid direct contact between the hot sintering parts and the water-cooled punches. This system can deliver a maximum load of 1.6 tons. A minimum value of 8 MPa is necessary at the beginning of the cycle to assure punch and samples contact.

The displacement of the punch, the applied pressure and the internal measured temperature are recorded as a function of time, allowing drawing *in-situ* dilatometric curves. The system can be controlled either manually (the operator chooses the delivered power and applied pressure), or in an automatic mode. In this case the thermo-mechanical cycle follows a pre-defined program of temperature-delivered power and applied pressure. In each case, tuning of resonance, by short-circuit punch position, and adaptation of the impedance are done manually.

To limit thermal losses, an aluminosilicate insulation box surrounds the sample. Two SiC plates (>99.9 % purity, from Umicore, Bagnolet, France), acting as susceptors, are disposed on each side of the sample and perpendicular to the microwaves propagation direction to initiate the heating. It is important to mention that the sintering is carried out in static air. Furthermore no mold was used in these experiments for two reasons (1) it is quite difficult to find a suitable material for molds, able to work in air, at high temperature and pressure in a microwave chamber, and presenting no (or slight) reactivity with the material. (2) It has been shown that spinel exhibits a pseudo-plastic behavior at high temperature [17] from which we can take advantage for the densification [18].

Using the as-defined assembly, the sample heating is provided by both thermal flux coming from the susceptors and dielectric microwave heating. This is the so-called hybrid heating mode. Images are extracted from the thermal camera and are displayed on figure 2. Those images show that (at the early stage of the process) the two SiC plates are first heated by microwaves (Fig.2.a) and transfer the heat to the sample by thermal radiation. Above approximately 1000°C, the dielectric losses of the spinel increase and it starts to heat by itself. On the photography, it can be seen that the spinel compact preferentially glows (fig. 2b), showing that the latter is being subjected to a hybrid heating process.

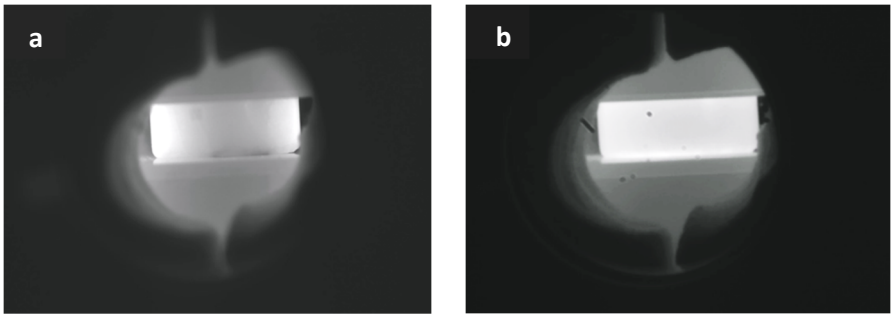

Fig. 2. Photography of a spinel sample showing radiative heating below 1000 °C from the SiC susceptors (a) and hybrid microwave heating over 1000 °C (b)

2.2. Sample Preparation

The starting material used in this study is a spinel $MgAl_2O_4$ provided by Solcera (Evreux, France), slip casted according to a proprietary method with S30CR powder from Baikowski (Poissy, France) (>99% purity, impurities are S 700 ppm, Na 41 ppm, Ca 15 ppm, Si 12 ppm, and Fe 6 ppm). The green samples are shaped in the form of small discs of 10 mm in diameter and 5 mm in thickness. The density was measured in ethanol by Archimedes method. The green samples were found to be close to 60% of theoretical density.

The green discs were polished in order to have two parallel faces. Then, a first heating is performed to sinter the material through the first stages of densification. The 8 MPa minimum starting value imposed by the hot press system, and the fact that no mold is used, imply that discs present initially a sufficient mechanical resistance for the upcoming microwave/press treatment. Samples were thus pre-sintered using a conventional furnace at 1400°C for 12 minutes, in air, with a heating rate of 10°C/min. This short heating cycle is sufficient to activate the densification mechanism, while limiting grain growth and avoiding intra-grain porosity entrapment. After this first densification step, the samples show density close to 90% TD, and their dimensions are about 8 mm of diameter, and 4 mm in thickness. Thereafter a final step of densification is carried out with microwave heating under a uniaxial pressure in order to remove all porosities and obtain transparency.

2.3. Temperature Calibration

As already mentioned, the temperature is measured by an infrared pyrometer pointing towards the sample surface, located in the center of the cavity. The low detection limit of this pyrometer is 250°C. No detail is given upon the value(s) of the emissivity coefficient used by the system. Using in-situ dilatometric curves, it has been experimentally observed that the shrinkage starts at a displayed temperature of ~1100°C, for an applied pressure of 25 MPa (Fig.4.a.). To evaluate the accuracy of the temperature measurement around that threshold point, a calibration test has been performed in the sintering conditions. Germanium oxide, which has a melting point of 1115°C, was chosen as a reference, following the procedure developed by Macaigne et al. [13]. This experiment was carried out by compacting GeO_2 powder on the side of a spinel disc, notched to hold the powder in place. The sample was then positioned at the center of the cavity as described earlier, with GeO_2 powder facing a CCD camera at the front side of the machine. This camera is used to record the time at which the melting occurs. At the same time, the infrared pyrometer measures the temperature at the back

side surface of the $MgAl_2O_4$ sample. The transverse view of the cavity is represented in Fig. 3. with both the CCD camera, and the pyrometer. Assuming the sample heats homogeneously and that the germanium oxide at the front side is at the same temperature as the spinel (or very close), the measured temperature can be compared to the expected melting temperature of GeO_2.

The observed melting temperature was 1117°C. As the theoretical melting point of germanium oxide is 1115°C, this experiment confirms a good estimation of the temperature value, at least in the range which is relevant for this study.

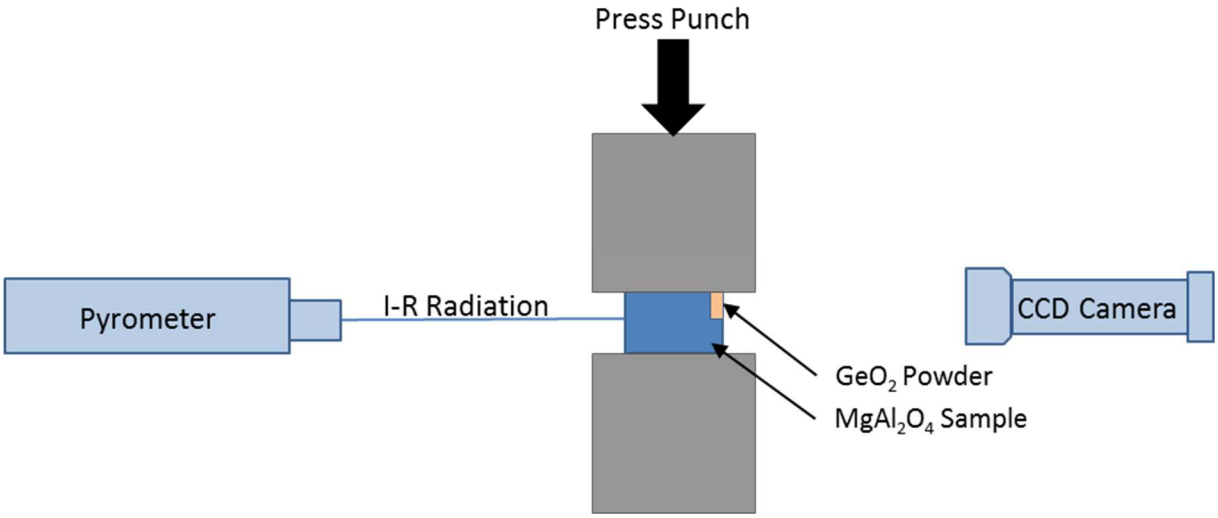

Fig. 3. Scheme of the experimental set-up for the temperature calibration test

2.4. Characterizations

The transmittance is measured using a Perkin Elmer lambda 1050 spectrophotometer, ranging from 1800 nm to 300 nm, with a detector change at 860 nm. This modification of detectors creates a measurement artifact, which is corrected using the visible detection as reference. The light is produced by a deuterium tungsten source. The measurement consists in comparing the intensity of two 3 mm wide square lasers, passing through two 2 mm wide circular holes. In a first time, an analysis with the sample support, but no sample is carried out to calibrate the machine. Then, the samples are placed on the side of the support, without moving it out of the machine. The measurement is performed within 5 to 6 minutes.

Transmittance measurement has been normalized to the same thickness (2 mm) to allow a comparison between samples. The following relations were used Eq.1-2 [13]:

$$IT2 = \frac{2n}{n^2+1} * \left(\frac{1}{IT1} * \frac{2n}{n^2+1}\right)^{-\frac{d2}{d1}} \quad (1)$$

Where IT_2 is in-line transmission for the corrected thickness (d_2 = 2 mm), and IT_1 is in-line transmission measured with real thickness d_1. Refraction index n is given by Sellmeier relation:

$$n^2 = 1 + \frac{1{,}8939\lambda^2}{\lambda^2 - 0{,}09942^2} + \frac{3{,}0755\lambda^2}{\lambda^2 - 15{,}826^2} \quad (2)$$

The determination of the grain size and the microstructures were obtained using a scanning electron microscope Zeiss supra 55, coupled with an EDAX EBSD detector. The sample surfaces were polished down to 1 µm with a diamond suspension, and 0.25 µm with colloidal silica. Since the spinel is insulating, the samples were glued to the support with a silver paint, which helped to evacuate the surface charges. Carbon coating was avoided in order to prevent pattern deterioration since EBSD characterization scans only the first 40 nm in depth [19]. The analysis was made with the sample tilted to 70° under the electron beam towards the EBSD detector, to maximize the data collection. The acquisition was made using the TSL OIM data Collection 6 software, and the results were interpreted using TSL OIM Analysis 6. The step between each measurement point was set to 50 nm, to have at least half a dozen points for each grain. The grain sizes were determined by an automatic intercept method from the software, using 40 horizontal lines.

Hardness and fracture toughness were evaluated using a micro-hardness tester Matsuzawa MMT-X7. A first set of ten indentations was realized with a weight of 1 kgf during 13 seconds on the surface of each sample to compare with results from the literature. The hardness is calculated by the Clemex software and is given in Vickers Hardness (HV). The obtained values were then averaged to get a better precision on the global hardness of the sample. The uncertainties have been calculated using the maximum and the minimum measured values on each sample.

For the fracture toughness, a similar protocol was followed. The half width of the indentation is then measured, as well as the length of the crack, with the same software that was used previously for the hardness. The crack pattern has been determined to be Palmqvist type by Sokol et al. [3]. The value of the tenacity has been calculated using the following equation (Eq.3. [3]) :

$$K_{1c} = 0.06 * \left(\frac{HvP}{4l}\right)^{\frac{1}{2}} \quad (3)$$

Where Hv the hardness in GPa, P the load in Newton (here equal to 9.807 N), and L the crack length in m.

3. Results and discussion

3.1. Sintering process

Using Spark Plasma Sintering on spinel, it has been shown that intermediate values of pressure (60 MPa < P < 80 MPa) and temperatures (1300°C < T < 1600°C) must be used to get transparent materials [20]. By analogy with this sintering technique under uniaxial pressure, similar experimental parameters were chosen as starting conditions here. Tests with pressure of 50 MPa and temperature up to 1100°C-1150°C were conducted. However, samples had been broken under such pressure, probably because no mold was used. The pressure was then gradually decreased through different tests down to 30 MPa. Moreover, to avoid cracking formation in the sample, it was necessary to apply it step by step and at a high temperature, around 900°C, and to remove the pressure at a similar temperature. This method allows the production of crack-free sintered spinel.

Through the observation of the dilatometric curves (Fig. 4.a), for pressure around 20 to 25 MPa, shrinkage starts at around 1100°C. This temperature corresponds to a 750 W delivered power for the

assembly and sample size used in this experiment. It must be noticed that using those conditions of temperature and pressure, a creeping mechanism can take place, which does not contribute here to the densification of the ceramics and may induce crack formation, due to cavitation. Therefore, the dwell times were kept short enough to limit this side effect. An optimal dwell time has been empirically determined by calculating the theoretical shrinkage to obtain 100% TD (assuming only axial shrinkage and no radial deformation). According to these criteria, we found an optimal protocol to get crack-free dense sample. The best chosen conditions are as follows: a dwell time of 8 min at 750 W and 30 MPa (Fig. 4.b).

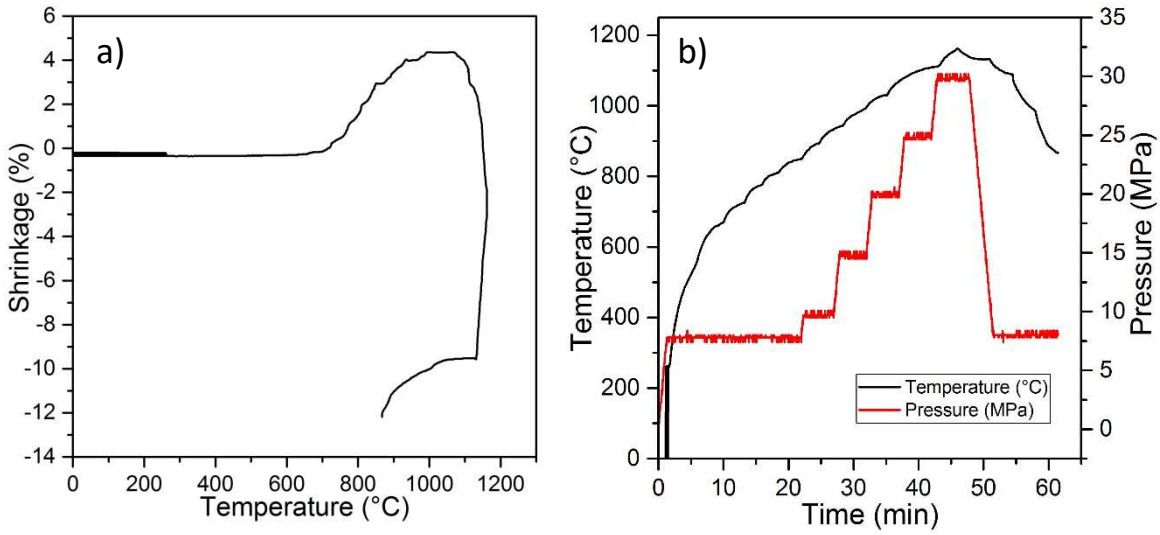

Fig. 4. a) In-situ dilatometric curve b) Temperature and pressure cycle for a 5 min dwell experiment

A thin white crown (less dense than in the center) can sometimes be visible on the periphery of the samples. The density gradient can be understood by two phenomena that are inherent to the technique. The first is the sample quite fast cooling from its surface by thermal radiation due to an imperfect thermal isolation. The second is the lack of radial constraints implying a pressure gradient from the center of the disk to its periphery.

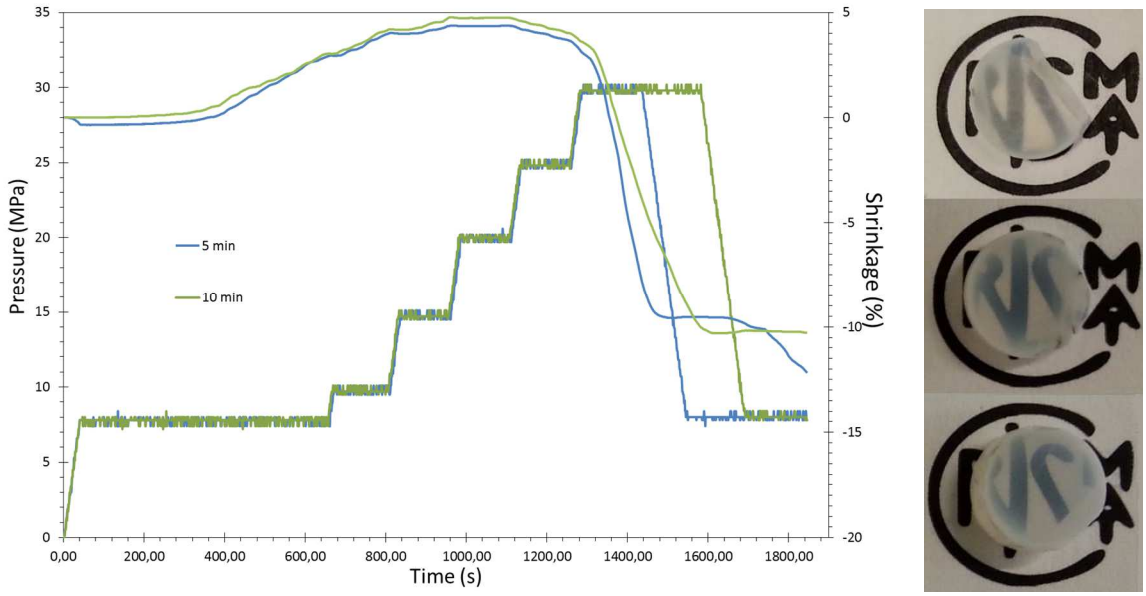

Fig. 5. Dilatometric curves as a function of time for corresponding dwell times, with corresponding samples in front of the CRISMAT logo. Samples are sorted from shorter to longer dwell time in descending order.

The impact of the dwell time on the physical properties of the spinel has been studied through three experiments performed with dwell times of 5, 8, and 10 min. After the experiment, the density of each sample was measured and found to be 100% of theoretical density. However, for a similar starting density, the total shrinkage is slightly higher for samples with longer dwell times (Fig.5.).

3.2. Characterization

3.2.1. Transmittance

During the measurement, two interfaces between spinel and air are crossed by the light beam. Those two interfaces, with abrupt change in refraction index, lead to a partial reflection of the laser (6-7% at each interface). This phenomenon implies a theoretical limit to the transmittance of 87% of light intensity without anti-reflect coating [21].

Figure 6 shows the value of the transmittance as a function of wavelength for the different samples. An artifact of measurement can be seen around 900 nm, due to the detector change during the analysis. It appears that an increase of the dwell time first improves the quality of the optical properties, with a higher transmittance in the IR domain for the 8 minutes dwell samples. Transmittance as high as 60 % at 600 nm, 77% at 1000 nm and 83% at 1600 nm have been obtained with this new method. Those transmittance results are similar to spinel sintered by SPS, but are still inferior to the results obtained by HIP densification in the visible range [20].

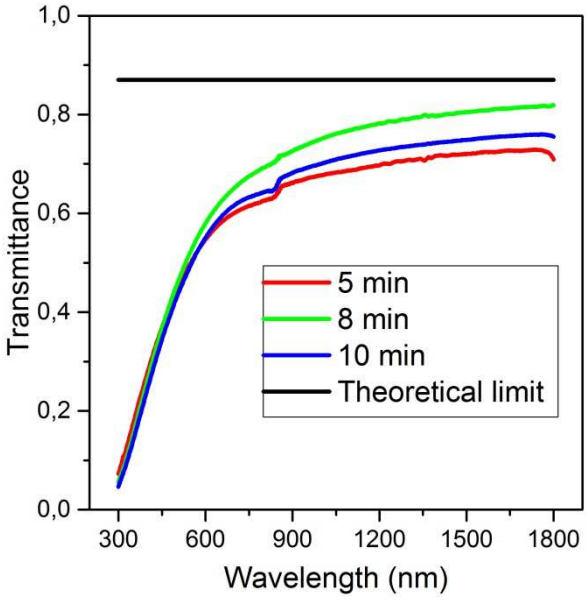

Fig. 6.Transmittance as a function of wavelength normalized for 2 mm thick samples: Impact of the dwell time on the quality of the transparency

It seems that there is an optimum sintering duration, since a dwell time of 10 min reduces the transmittance by 5 to 10 % for 2 mm thick samples, as can be seen on Fig.6. This optimum might be explained by the sintering method used in this experiment. Grains sliding mechanism takes place through the creeping phenomena, in resulting the pores formation by cavitation for longer dwell times [14].

Even if the measurement of density by Archimedes method in ethanol gave a density of ~ 100%, there is still some residual porosity in the samples. This remaining porosity can explain the decrease of transmittance in the visible range. It has been shown that with 0.05% of pores 100 nm wide, transmittance is reduced by half at 600 nm [21]. Furthermore, with 0.05% of porosity, the diameter of the pores must be less than 20 nm to not affect the in-line transmittance [21]. However, it has not been possible to measures either the amount of porosity nor the sizes of the pores in this work.

3.2.2 Grain size

To control if the heating has been homogeneous, measurements were done at different areas from the middle of the discs to the edge. No significant difference in microstructure or in grain size has been observed in function of the position, confirming that the volume heating has occurred and that the samples are homogeneous.

A typical result of EBSD analysis on the spinel samples studied here is shown in Fig. 7. with an auto grain and an IQ with a measurement done on the sample which was subject to a 5 min dwell time. The mean grain size measured for the samples with 5 and 8 min dwell time is 0.45 and 0.5 $\pm$ 0.05 µm, and for the sample with 10 min, the mean grain size is 0.55 $\pm$ 0.05 µm. This process seems consistent for the production of transparent spinel with sub-micron grain size. The short stage at high temperature combined with pressure is likely responsible for this observed limited grain growth.

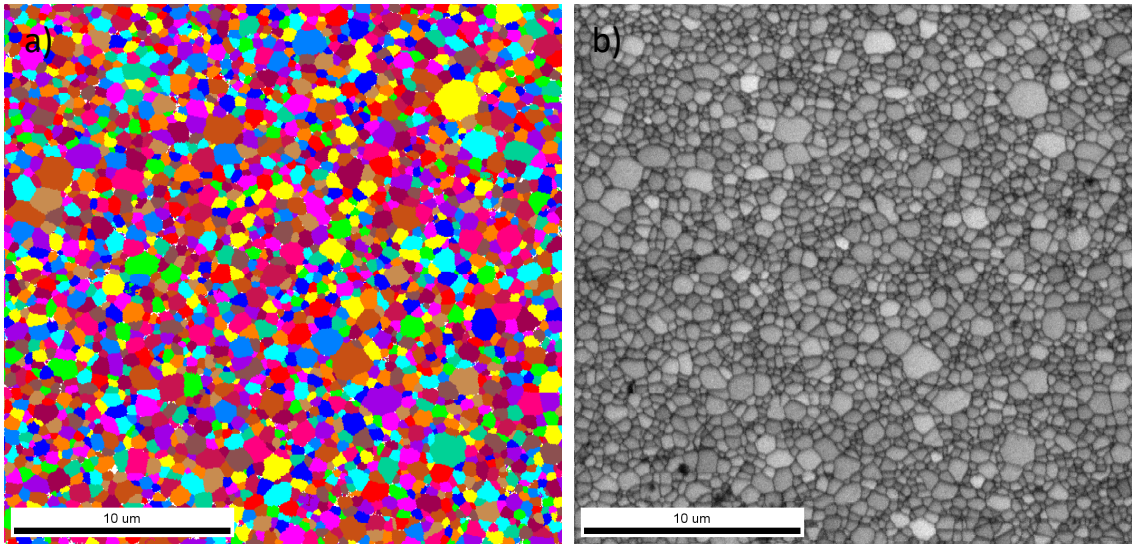

Fig. 7. a) Auto grain image generated with EBSD data of a transparent spinel b) IQ image generated by OIM

The submicron grain size obtained here should have a good impact on the mechanical properties of this material. Hence, the hardness and fracture toughness were characterized on these three samples.

3.2.3 Hardness and fracture toughness

Figure 8 shows the results of mechanical characterizations. For comparison, dash lines figuring the results from the literature in the same measurement conditions have been drawn [3, 5].

Hardness values are ranging from 17 to 15 GPa depending on the dwell time (Fig.8.). Hardness decreases with longer dwell time, which is consistent with the greater grain sizes observed. Fracture toughness is almost constant whatever the dwell time, and remains close to values reported in the literature on HIPed samples [3, 5].

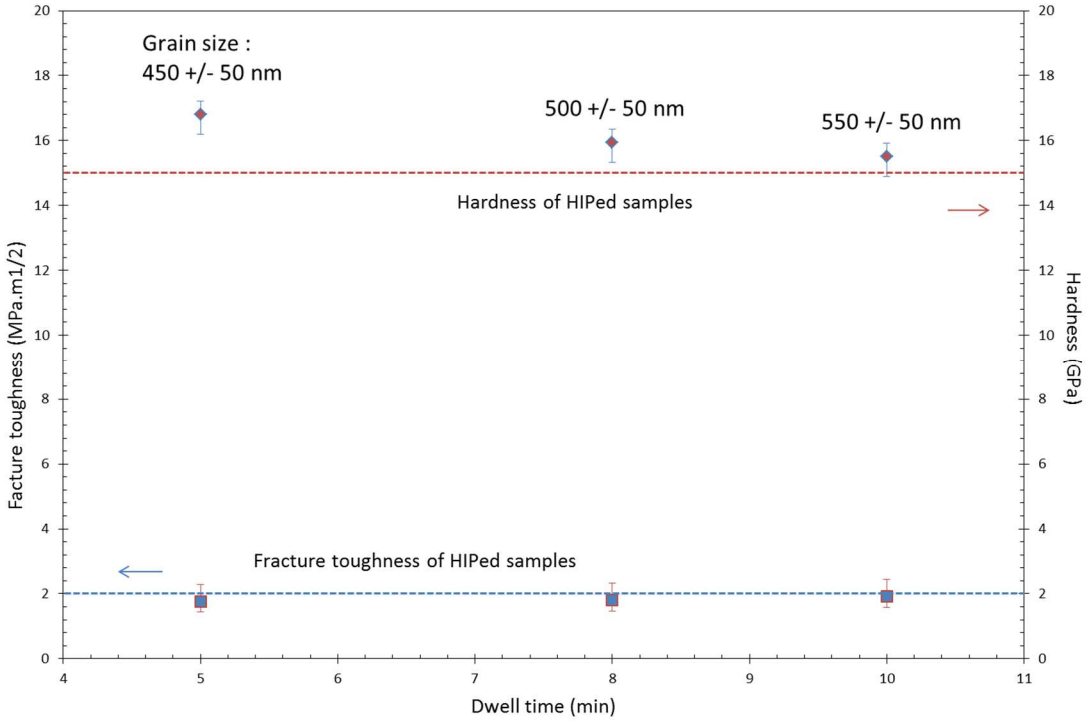

Fig. 8. Hardness and fracture toughness depending on dwell time compared to HIPed references

Overall, mechanical properties are similar to those measured for HIPed samples. However, long sintering time presents two major drawbacks. The first is obviously the grain growth, and the second is the creation of porosity due to grains sliding, which alters the optical properties.

4. Conclusion

Sub-micrometric transparent polycristalline spinel $MgAl_2O_4$ has been obtained in a short thermal process (8 minutes dwell time at the high temperature stage) using a new microwave pressure-assisted system. Inspired from sinter-forging and adapted to the microwave furnace, this process was successfully used to produce samples with high transmittance values and high mechanical properties due to sub-micrometric grain size. This new technique allows the production of transparent spinel in air, with a transmittance up to 83 % in the IR range.

Acknowledgement

The authors would like to thank Solcera for the samples, and the Labex for the financial support. The authors are also thankful to Jerome Lecourt and Jean-Pierre Burnouf for their precious help in conducting the experiments.

References

[1]. S.F. Wang, J. Zhang, D.W. Luo, F. Gu, D.Y. Tang, Z.L. Dong, G.E.B. Tan, W.X. Que, T.S. Zhang, S.Li, L.B. Kong, Transparent Ceramics: Processing, Materials and Applications, *Prog. in Solid State Chem.* 41 (2013) 20-54.

[2]. J. Petit, L. Lallemant, Drying step optimization to obtain large-size transparent magnesium-aluminate spinel samples, *Proc. SPIE 10179, Window and Dome Technologies and Materials XV,* 101790K (2017).

[3]. A. Krell, J.Klimke, T. Hutzler, Advanced Spinel and Sub-Um Al_2O_3 for Transparent Amor Applications, *J. Am. Ceram. Soc.* 29 (2009) 275-81.

[4]. A. Sutorik, G. Gilde, J. Swab, C. Cooper, R. Gamble, E. Shanholtz, The Production of Transparent MgAl2O4 Ceramic Using Calcined Powder Mixtures of Mg(OH)2 and c-Al2O3 or AlOOH, *Int. J. Appl. Ceram. Technol.* 9 (2012) 575–587

[5]. A. Goldstein, A. Goldenberg, M. Hefetz. Transparent Polycrystalline MgAl2O4 Spinel with Submicron Grains, by Low Temperature Sintering . *J. Ceram. Soc. Jpn* 117 (2009) 1281-83.

[6]. K. Morita, B.-N. Kim, H. Yoshida, K. Hiraga., Spark-Plasma-Sintering Condition Optimization for Producing Transparent $MgAl_2O_4$ Spinel Polycrystal, *J. Am. Ceram. Soc.* 92 (2009) 1208-16.

[7]. G. Bonnefont, G. Fantozzi, S. Trombert, L. Bonneau., *Fine-Grained Transparent $MgAl_2O_4$ Spinel Obtained by Spark Plasma Sintering of Commercially Available Nanopowders*, *Ceram. Int.* 38 (2012) 131-40.

[8]. M. Sokol, M. Halabi, S. Kalabukhov, N. Frage, Nano-Structured MgAl 2 O 4 Spinel Consolidated by High Pressure Spark Plasma Sintering (HPSPS), *J. Eur. Ceram. Soc.* 37 (2017) 755-62.

[9]. K. Morita, B.-N. Kim, K. Hiraga, H. Yoshida, Fabrication of Transparent MgAl2O4 Spinel Polycrystal by Spark Plasma Sintering Processing , *Scr. Mater.* 58 (2008) 1114-17.

[10]. L.L. Zhu, Y.J. Park, L. Gan, S.-I. Go, H.N. Kim, J.M. Kim, J.W. Ko, Fabrication of Transparent MgAl 2 O 4 from Commercial Nanopowders by Hot-Pressing without Sintering Additive, *Mater. Lett.* 219 (2018) 8-11.

[11]. A. Krell, J. Klimke, T. Hutzler. Transparent Compact Ceramics: Inherent Physical Issues, *Opt. Mater.* 31 (2009) 1144-50.

[12]. G. Bernard-Granger, N. Benameur, C. Guizard, M. Nygren, Influence of Graphite Contamination on the Optical Properties of Transparent Spinel Obtained by Spark Plasma Sintering, *Scr. Mater.* 60 (2009) 164-67.

[13]. R. Macaigne, S. Marinel, D. Goeuriot, C. Meunier, S. Saunier, G. Riquet, Microwave Sintering of Pure and TiO2 Doped MgAl2O4 Ceramic Using Calibrated, Contactless in-Situ Dilatometry, *Ceram. Int.* 42 (2016) 16997-3.

[14]. D. Agrawal, Latest Global Developments in Microwave Materials Processing, *Mater. Res. Innov.* 14, (2010) 3-8.

[15]. G. Riquet, S. Marinel, Y. Breard, C. Harnois, A. Pautrat., Direct and Hybrid Microwave Solid State Synthesis of CaCu3Ti4O12 Ceramic: Microstructures and Dielectric Properties, *Ceram. Int.* 44 (2018) 15228-35.

[16]. M. Oghbaei, O. Mirzaee, Microwave versus Conventional Sintering: A Review of Fundamentals, Advantages and Applications, *J. Alloy. Compd.* 494 (2010) 175-89.

[17]. F. Beclini, R. Duclos, J. Crampon, F. Valin, MICROSTRUCTURAL SUPERPLASTIC DEFORMATION IN MgO • A1203 SPINEL, Acta metal. Mater. 43 (1995) 2753-60

[18]. R. L. Coble, Diffusion Models for Hot Pressing with Surface Energy and Pressure Effects as Driving Forces, *J. Appl. Phys.* 41 (1970) 4798-4807.

[21]. N. Benameur, Elaboration et caractérisations d'un spinelle polycristallin à grains fins transparent dans le visible et l'infrarouge, 2009, 198.

[19]. D. Dingley, Progressive Steps in the Development of Electron Backscatter Diffraction and Orientation Imaging Microscopy: EBSD AND OIM, *J. Microsc.* 213 (2004) 214-24.

[20]. M. Rubat du Merac, H.J. Kleebe, M.M. Müller, I.E. Reimanis, Fifty Years of Research and Development Coming to Fruition; Unraveling the Complex Interactions during Processing of Transparent Magnesium Aluminate ($MgAl_2O_4$) Spinel, *J. Am. Ceram. Soc.* 96 (2013) 3341-65.

[21]. T. Benitez, S.Y. Gómez, A.P. Novaes de Oliveira, N. Travitzky, D. Hotza, Transparent Ceramic and Glass-Ceramic Materials for Armor Applications, *Ceram. Int.* 43 (2017) 13031-46.